Dual action heteromultivalent glycopolymer stringently block and arrest influenza A virus infection in vitro and ex vivo

Journal:	*Nano Letters*
Manuscript ID	nl-2023-004082
Manuscript Type:	Communication
Date Submitted by the Author:	01-Feb-2023
Complete List of Authors:	Parshad, Badri; Wellman Center for Photomedicine, Stadtmüller, Marlena; Robert Koch Institut, Unit 17, Influenza and Other Respiratory Viruses Baumgardt, Morris; Universitätsklinikum Carl Gustav Carus, Medical Clinic III, Devision of Nephrology Ludwig, Kai; Freie Universitat Berlin Fachbereich Biologie Chemie Pharmazie, Chemie Nie, Chuanxiong; Freie Universitat Berlin, Department of Chemistry and Biochemistry; Freie Universitat Berlin, Institut für Virologie Rimondi, Agustina; Robert Koch Institut, Unit 17, Influenza and Other Respiratory Viruses Hönzke, Katja; Universitätsklinikum Carl Gustav Carus, Medical Clinic III, Devision of Nephrology Angioletti-Uberti, Stefano; Imperial College London, Department of Materials Khatri, Vinod; Freie Universität Berlin Schneider, Paul; DRK Kliniken Berlin, Department for Thoracic Surgery Herrmann, Andreas; Freie Universität Berlin Haag, Rainer; Freie Universitat Berlin, Institut für Chemie und Biochemie Hocke, Andreas; Charité Universitätsmedizin Berlin, Department of Infectious Diseases and Respiratory Medicine Wolff, Thorsten; Robert Koch Institute, Infectious Diseases Bhatia, Sumati; Freie Universität Berlin, Chemistry and Biochenistry

Dual action heteromultivalent glycopolymer stringently block and arrest influenza A virus infection *in vitro* and *ex vivo*

*Badri Parshad,[a,b] Marlena N. Stadtmüller,[c,d] Morris Baumgardt,[e] Kai Ludwig,[f] Chuanxiong Nie,[a] Agustina Rimondi,[c] Katja Hönzke,[e] Stefano Angioletti-Uberti,[g] Vinod Khatri,[a] Paul Schneider,[h] Andreas Herrmann,[a] Rainer Haag,[a] Andreas Hocke,[e] Thorsten Wolff,[c] Sumati Bhatia[a]**

[a]Institut für Chemie und Biochemie Organische Chemie, Freie Universität Berlin, Takustr. 3, 14195 Berlin, Germany

[b]Wellman Center for Photomedicine, Massachusetts General Hospital, Harvard Medical School, Boston, MA 02129, USA

[c]Unit 17, Influenza and Other Respiratory Viruses, Robert Koch-Institut, Seestraße 10, 13353 Berlin, Germany

[d]Medical Clinic III, Devision of Nephrology, Universitätsklinikum Carl Gustav Carus, Fiedlerstr. 40, 01307 Dresden, Germany

[e]Department of Infectious Diseases and Respiratory Medicine, Charité - Universitätsmedizin Berlin, corporate member of Freie Universität Berlin, Humboldt-Universität zu Berlin, and Berlin Institute of Health, Berlin, Germany

[f]Forschungszentrum für Elektronenmikroskopie and Core Facility BioSupraMol, Institut für Chemie und Biochemie, Freie Universität Berlin, Fabeckstr. 36a, 14195 Berlin, Germany

[g]Department of Materials, Imperial College London, London, UK

[h]Department for Thoracic Surgery, DRK Clinics, Berlin, Germany

ABSTRACT

Here, we demonstrate concerted inhibition of different influenza A virus (IAV) strains using a low molecular weight dual-action linear polymer. The 6´-sialyllactose and zanamivir conjugates of linear polyglycerol are optimized for simultaneous targeting of hemagglutinin and neuraminidase on the IAV surface. Independent of IAV subtypes, hemagglutination inhibition data suggest better adsorption of heteromultivalent polymer than homomultivalent analogs onto the virus surface. Cryo-TEM images imply heteromultivalent compound-mediated virus aggregation. The optimized polymeric nanomaterial inhibits >99.9% propagation of various IAV strains 24 hours post-infection *in vitro* at low nM concentrations and is up to 10000 times more effective than the commercial zanamivir drug. In a Human Lung *ex vivo*-multicyclic infection setup, the heteromultivalent polymer outperforms the commercial drug zanamivir, and homomultivalent analogs or their physical mixtures. This study authenticates the translational potential of the dual action targeting approach using small polymers for broad and high antiviral efficacy.

Keywords: Heteromultivalency, influenza A virus, dual-action linear polymer, multicyclic infection, broad inhibition

Influenza A viruses (IAV) regularly challenge public health globally by causing seasonal influenza and sporadic pandemics leading to 3-5 million cases of severe illness and an estimated 290,000 to 650,000 deaths per year worldwide.[1] The unpredictable patterns of IAV antigenic drift and shift make the annual adaptation of vaccines challenging. Also, recent studies have illustrated that influenza A virus co-infection may enhance the severity of concomitant COVID-19.[2–4]

The IAV is an enveloped RNA virus whose membrane anchors two surface proteins, the homotrimeric hemagglutinin (HA) that binds to sialic acid (SA) on cell surfaces and the tetrameric neuraminidase (NA) which is a sialidase responsible for cleaving sialoside bonds between HA and SA .[5–8] The process of IAV binding to host cell receptors is highly dynamic, and before ultimately being internalized, virus particles move along the host cell membrane.[9] This process is facilitated by the multivalent attachment of multiple noncovalent HA-SA bonds that in turn can be cleaved by NA, resulting in a directional movement.[10–12]

The NA also allows virions to move through the host mucus layer which is rich in sialylated glycoproteins. These sialylated glycoproteins otherwise could inhibit viral entry into the host system.[13] Overall, the balance of HA receptor-binding and NA receptor-cleaving activity is pivotal for virus replication and transmission. Commercial anti-influenza drugs such as Oseltamivir and Zanamivir are NA inhibitors that can prevent the cleavage of sialoside bonds with HA proteins, thus able to interfere with the mobility as well as the release of newly formed virions from the host cell and consequently, the propagation of viral infection.[14] The emergence of stable and transmissible drug resistance in IAV strains can render these drugs ineffective as suggested by oseltamivir and zanamivir-resistant IAVs.[15]

Inhibiting the infection at an early step by targeting the HA to prevent binding and subsequent entry of the virus into the target cell is a promising approach. Multivalent sialoside-based polymers,[16] dendrimers,[17] nanoparticles,[18,19] nanogels,[20,21] and proteins[22] have overcome the low binding affinity (Kd ~ 2-4 mM)[23] of monovalent SA to HA through a multivalent effect and have shown significant inhibition of IAV binding to the host cells. However, due to the rather high amino acid sequence and structural variability of the HA binding pocket of different strains, broad activity with high efficacy is still elusive for most polysialylated inhibitors.[24,25] Replacing SA with

6´-sialyllactose (SL), which mimics the natural receptor more closely, extended the activity against some IAV strains; high potency, however, remained a bottleneck.[24]

Through a careful design, we have overcome this challenge by developing a heteromultivalent linear polyglycerol (LPG) with zanamivir (ZA) and 6´-sialyllactose (SL) residues, which is highly potent and broadly active against IAV infection. We have chosen 10 kDa LPG for multivalent display because of its excellent water solubility, cytocompatibility, scalability, and good *in vivo* clearance.[25,26] The optimized heteromultivalent presentation of SL and ZA generated a broad activity against different IAV strains. This compound broadly inhibits IAV propagation *in vitro* and in human lung (HuLu) explants at a low nM concentration and is also three to four orders of magnitude more potent at inhibiting IAV propagation than the commercially available ZA drug. This detailed investigation emphasizes heteromultivalency and suggests synergistic effects against both the binding and release of various IAVs for the first time using a low molecular weight biocompatible polymer.

Considering the uniform distribution of 300-500 HA trimers[27,28] on the IAV surface, we have optimized the SA ligand density on the 10 kDa LPG scaffold as 40-70% for an effective IAV inhibition in our previous reports.[25] Accordingly, SA and SL with 40% and 50% degree of functionalization (DF), respectively, on LPG was selected here as homomultivalent ligands for targeting the HA protein. Contrary to HA, the distribution of NA on IAV surface is not uniform and highly variable. The tetrameric NAs are usually present on the virus surface as clusters of two or more proteins[28] and the previous reports showed that up to 10% ZA on a polymer backbone is enough to afford an effective inhibition of virus release from the cell surface.[29] We therefore prepared homomultivalent ZA on LPG with low (10%) and medium (40%) DFs i.e., $LPG_{10}ZA_{0.10}$ and $LPG_{10}ZA_{0.40}$, respectively. To investigate a favorable configuration for effective virus

inhibition in the dual action mode, LPG with optimum SA or SL density and a variable degree of ZA functionalization were synthesized. Essential steps for the synthesis of ZA-alkyne are shown in **Scheme 1A** (complete syntheses of ZA-alkyne and SL-alkyne are shown in **Scheme S1** and **S2**). The DFs of each ligand on the heteromultivalent constructs correspond to the DF on the homomultivalent constructs to afford three heteromultivalent compounds i.e., $LPG_{10}ZA_{0.10}SA_{0.40}$, $LPG_{10}ZA_{0.10}SL_{0.40}$, and $LPG_{10}ZA_{0.40}SL_{0.40}$ (**Scheme 1B-C**, See supporting for synthesis details). The loading of ZA and SA or SL ligands was determined by ^{1}H NMR analysis for different compounds and the zeta potential of polymer conjugates was measured in PB (10 mM, pH 7.4) at the concentration of 1 mg/mL.

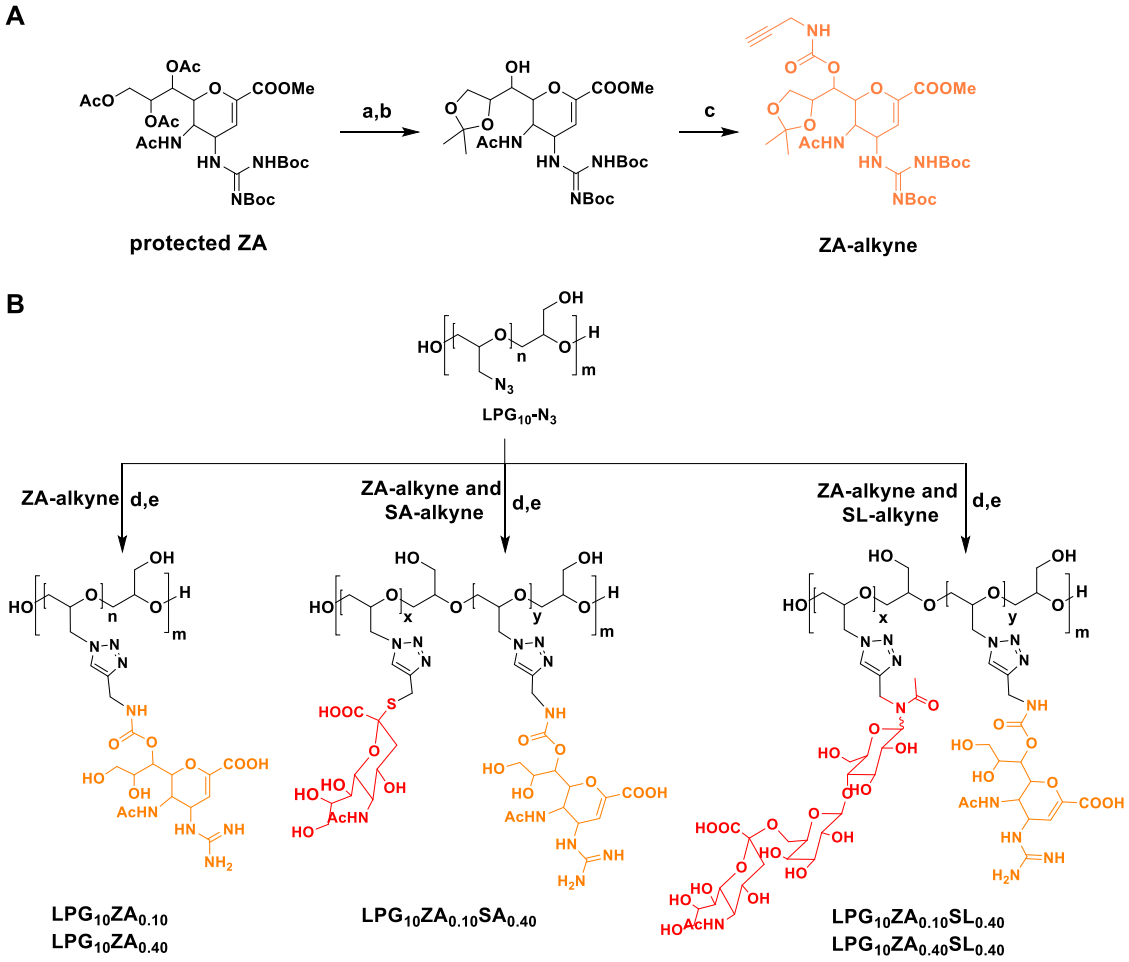

C

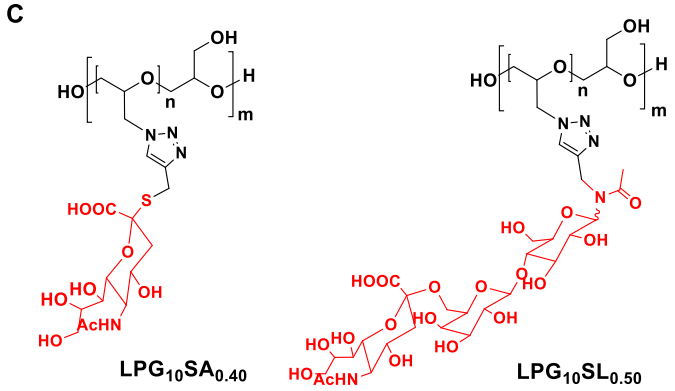

Scheme 1. (A) Important steps for the synthesis of ZA-alkyne while the complete synthesis is shown in **Scheme S1**. Reagent and conditions: (a) NaOMe, MeOH, rt, 4 h; (b) acetone, triflic acid, rt, 4 h; (c) *p*-nitrophenyl chloroformate, pyridine, DMAP, propargylamine, rt, 16 h. (B) Synthesis of ZA, SA, and SL-functionalized linear polyglycerol polymers. Reagent and conditions: (d) ZA/SA/SL, $CuSO_4.5H_2O$, sodium ascorbate, DMF:H_2O, 50 ^oC, 48 h; (e) (i) 2M aq. NaOH, rt, 5 h (ii) DCM, TFA, rt, 5 h. (C) Structures of SA and SL functionalized linear polyglycerols.

Table 1. Characterization of all compounds tested against A/X31 (H3N2) virus.

Polymer[a] ($LPG_{10}ZA_{DF}SA_{DF}$)	**DF[b] (%)**	**SA/SL & ZA per polymer[c]**	**ζ-potential ±SD [mV][d]**	**NA inhibition IC_{50}±SD [nM] [ZA][e]**
$LPG_{10}OH$	-	-	-2.7±1.66	1775 ± 592
$LPG_{10}SA_{0.40}$	SA = 44	SA = 60	-30.8±2.58	1579 ± 336
$LPG_{10}SL_{0.50}$	SL = 50	SL = 67	-18.6±1.72	>10 000
Zanamivir	-	-	-	0.97 ± 0.16
$LPG_{10}ZA_{0.10}$	ZA = 10	ZA = 13	-3.3±1.40	2.10 ± 0.41 (27.3)
$LPG_{10}ZA_{0.40}$	ZA =40	ZA = 54	-17.4±3.48	1.27 ± 0.24 (68.58)
$LPG_{10}ZA_{0.10}SA_{0.40}$	ZA = 13, SA = 40	ZA = 20, SA = 54	-29.5±4.34	0.07 ± 0.01 (1.4)
$LPG_{10}ZA_{0.10}SL_{0.40}$	ZA = 10, SL = 40	ZA = 13, SA = 54	-22.4±3.66	19.58 ± 4.76 (255)
$LPG_{10}ZA_{0.40}SL_{0.40}$	ZA = 40, SL = 40	ZA = 54, SL = 54	-15.9±4.95	4.86 ±1.25 (262)

[a]The number of sialic acid (SA), 6´-sialyllactose (SL), and zanamivir (ZA) unit per hydroxyl group of LPG polymer of 10 kDa as calculated using a degree of functionalization (DF). [b]Determined by ^{1}HNMR analysis. [c]Number of sialic acid (SA), 6´-sialyllactose (SL), and zanamivir (ZA) units per polymer was calculated from DF by ^{1}HNMR. [d]The zeta (ζ)-potential was measured in PB (10 mM, 7.4 pH) at 1 mg/mL of concentration. [e]The IC_{50} in terms of ZA conjugated with the polymer backbone is given in brackets. Values are obtained by MUNANA assay with A/X31 (H3N2) virus. Values are expressed as mean ±SD, n=6.

We first tested NA inhibition activity of all compounds against A/X31 (H3N2) virus in a standard fluorescence-based assay using 2′-(4-Methylumbelliferyl)-α-D-*N*-acetylneuraminic acid

(MUNANA) (**Table 1** and **Figure 1A**). The multivalent ZA compounds with different loadings of ZA alone ($LPG_{10}ZA_{0.10}$ and $LPG_{10}ZA_{0.40}$) or in combination with SA ($LPG_{10}ZA_{0.10}SA_{0.40}$) showed very low IC_{50} values in the nanomolar range (1.4–68.6 nM ZA). Interestingly, $LPG_{10}ZA_{0.10}SL_{0.40}$ and $LPG_{10}ZA_{0.40}SL_{0.40}$, with SL and ZA, showed weak NA inhibition (IC_{50} > 250 nM ZA), almost 180 times less efficient than the corresponding $LPG_{10}ZA_{0.10}SA_{0.40}$ (IC_{50} ~ 1.4 nM ZA). This might be due to the reduced accessibility of randomly distributed ZA residues to the NA enzyme receptor pocket in presence of the bulky trisaccharide units of SL residues on the same polymer chain. In this assay, where NA inhibition values solely depend on the NA binding, monovalent ZA has better NA inhibition than the multivalent analogs. These results might be attributed to the higher conformational entropic cost of grafted ZAs compared to free monovalent ZA ligands for making bound ZA-NA interaction pairs, as previously observed by others.[30] Importantly, the control compound $LPG_{10}OH$ and sialic acid-based inhibitors $LPG_{10}SA_{0.40}$ and $LPG_{10}SL_{0.40}$ did not show any inhibition of NA activity.

The next step was to test the potential of these compounds as inhibitors of virus-cell binding. The hemagglutination inhibition (HAI) assay was performed with different compounds using influenza A viruses A/X31 (H3N2), A/Panama/2007/1999 (H3N2), A/Bayern/63/2009 (H1N1pdm) and A/California/7/2009 (H1N1pdm) (**Figure 1B**). The homomultivalent SA analog $LPG_{10}SA_{0.40}$ showed weak inhibitory activity only against H3N2 viruses whereas $LPG_{10}SL_{0.40}$ showed strong inhibition (Ki = 625 nM) also of the A/Bayern/63/2009 (H1N1pdm) virus. We expect an extended chain conformation of linear polyglycerol when conjugated with the trisaccharide SL ligands, and thereby reducing the conformational penalty of the polymer for adsorption onto the virus surface as compared to the globular $LPG_{10}SA_{0.40}$. Important to notice, no globular morphologies were seen for $LPG_{10}SL_{0.50}$ in cryo-TEM (**Figure S16**). The heteromultivalent analog $LPGZA_{0.40}SL_{0.40}$

showed broad HA inhibition with low nM inhibition constants (Ki) against all the tested IAV strains (**Table S1**). The ZA functionalized inhibitors ($LPG_{10}ZA_{0.10}$ and $LPG_{10}ZA_{0.40}$) showed little or no HA inhibition, and the heteromultivalent combination of ZA and SA ($LPGZA_{0.10}SA_{0.40}$) inhibited hemagglutination substantially better than the homomultivalent SA ($LPG_{10}SA_{0.40}$) only against IAV A/X31 (H3N2). These data clearly show that the presence of ZA ligands makes some ZA-NA ligand pairs that facilitate the polymer adsorption onto the virus surface, leading to better virus blocking and thus inhibition. As described earlier, the multivalent polymer adsorption onto the receptor-coated virus surface is very much dependent on the conformation penalty of polymer and ligand-receptor pair interactions upon binding.[30,31] No HA inhibition was observed with control compounds $LPG_{10}OH$, Zanamivir, and 6´-sialyllactose up to the concentration range of 10^4-10^5 nM (**Table S1**).

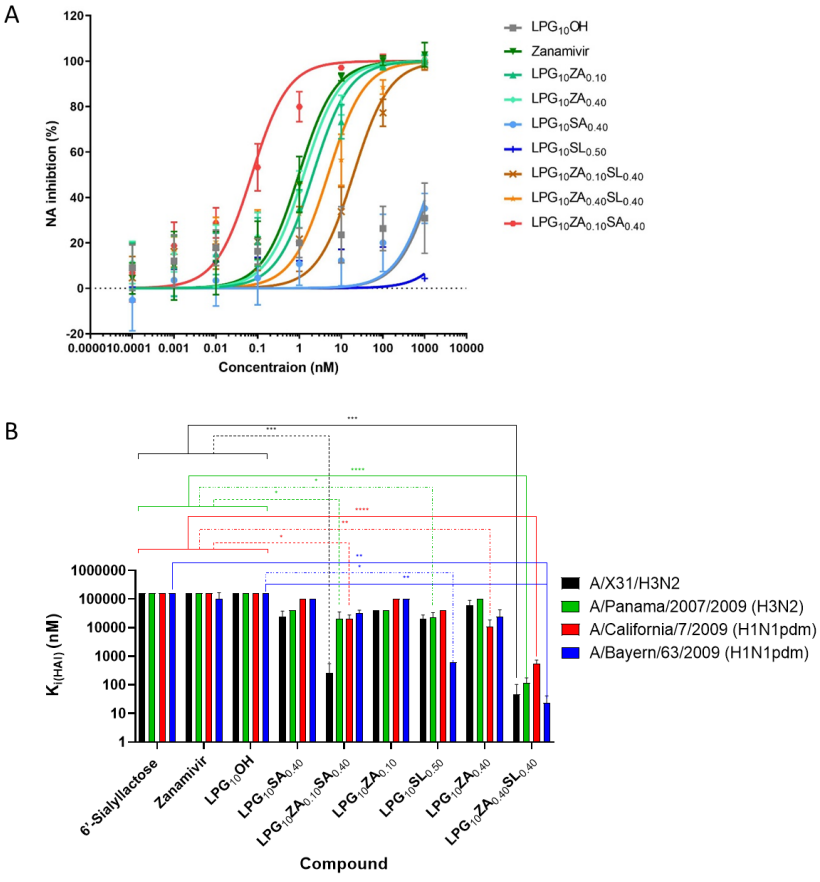

Figure 1. (A) NA inhibitory activity of the compounds by MUNANA assay. Values are expressed as mean ±SD, n=6. (B) Inhibitory effect of compounds tested against different IAV subtype strains. The inhibitor constant $K_{i(HAI)}$ was calculated and presented as log10 $K_{i(HAI)}$ for better visualization. The $K_{i(HAI)}$ reflects the lowest inhibitor concentration necessary to achieve full inhibition of virus-induced hemagglutination. The graph shows the mean and standard deviation (SD) of three independent experiments with each virus. *p*-values were determined using ANOVA with multiple testing (Kruskal-Wallis test and Dunn's test).

To analyze and compare the broad therapeutic activity of different homo- and heteromultifunctional compounds against virus propagation in a multicyclic infection setup, we have here included the more recent virus of the H3N2 subtype i.e. A/Panama/2007/2009 (H3N2) and the pandemic H1N1 virus A/Bayern/63/2009 (H1N1pdm), which diverge greatly from X/31 (H3N2) virus on the HA and NA amino acid sequence to represent a broad variety of IAV strains (**Figure 2**). Compounds at different dilutions were incubated with Madin-Darby Canine Kidney **(**MDCK-II) cells after establishing infection with the virus for 45 min at MOI 0.01. At 24 hpi, the virus titer in the supernatant was analyzed by plaque assay. The control compound $LPG_{10}OH$ did not show inhibition of virus propagation even at 1 or 10 µM and SA-functionalized $LPG_{10}SA_{0.40}$ was active only against A/X31 (H3N2) virus with an IC_{50} of 31 nM (~ 1870 nM SA). A broader antiviral activity was observed by replacing SA with SL residues that closely mimics the canonical receptor for IAV,[32] but IC_{50} values increased to 600–2800 nM. Commercially available monovalent ZA showed broad but quite weak antiviral activity against all three strains with IC_{50} values in the µM range (6.5–9.9 µM). On the other hand, the multivalent ZA compounds $LPG_{10}ZA_{0.10}$ and $LPG_{10}ZA_{0.40}$ showed nanomolar IC_{50} values against A/X31 (H3N2) (6 and 3 nM) and A/Panama/2007/1999 (H3N2) (58 and 45 nM) but very high µM IC_{50} values against the A/Bayern/63/ 2009 (H1N1pdm) (77 and 14 µM). These experiments were conducted on MDCK-II cells, which express low levels of α2,6-linked Neu5Ac, the host cell receptor of human IAVs. Thus, there are fewer glycan receptors to retain progeny virus at the cell surface, and therefore

influenza viruses are less dependent on NA activity in this setting.[33] Increased antiviral activity of multivalent ZA compared to monovalent ZA against A/X31 and Panama strains under these conditions is intriguing, especially considering the weaker NA inhibition activity of multivalent than the monovalent ZA (**Table 1**). These findings suggest that steric effects play a role in addition to the inhibition of NA by the multivalent ZA compounds, where the polymer bound to NA through ZA might sterically hinder the attachment of the virus to host cells.

Using dual action inhibitors with both ZA and SA or SL on the same polymer chain effectively increased the inhibition of virus propagation as indicated by a dramatic decrease in the IC_{50} values. The compound $LPG_{10}ZA_{0.10}SA_{0.40}$ demonstrated broad antiviral activity in a nM range against all three strains 0.2–156 nM (corresponding to 2 nM–2 µM ZA). Furthermore, using SL residues instead of SA in combination with ZA ($LPG_{10}ZA_{0.40}SL_{0.40}$) further decreased the IC_{50} values to 0.7–2.0 nM (corresponding to 35–128 nM of ZA). Interestingly, the dose-response curves for the virus propagation indicated that in comparison to homomultivalent ZA analogs, the heteromultivalent SA and ZA improved the inhibition of propagation of A/Panama/2007/1999 (H3N2) virus slightly, and A/Bayern/63/2009 (H1N1pdm) virus significantly, although these viruses were not as much inhibited by the homomultivalent sialoside compound (**Figure 2B-C**). This may in part be explained by an earlier observation for A/Panama/2007/1999 (H3N2) virus showing that multivalent SA-functionalized polyglycerols can bind to virions without inhibiting their propagation.[24] The SA-supported binding of heteromultivalent LPG may contribute to a higher surface concentration of ZA and thus to an enhanced inhibitory effect of ZA.

Intriguingly, dose-response curves are much steeper with the application of SL-containing compounds $LPG_{10}ZA_{0.40}SL_{0.40}$ and $LPG_{10}SL_{0.50}$ for A/Panama/2007/1999 (H3N2) and A/Bayern/63/2009 (H1N1pdm) viruses. For the A/X31 virus, the application of homomultivalent

SA compound $LPG_{10}SA_{0.40}$ resulted in steeper dose response curve than the $LPG_{10}SL_{0.50}$ (**Figure 2A-C**). This difference in steepness in the dose-effect curves cannot be attributed to different degrees of ligand conjugation, as they are similar or at least in the same range for all compounds. It is conceivable that the length of the trisaccharide SL linker might also enhance the number of interacting HA molecules that are not accessible to a sole monosaccharide SA functionalization. In addition, SLs of the LPG not engaged in HA interaction may protrude from the viral surface and therefore may add to the steric inhibition.[34,35]

The IC_{50} values of monovalent and homomultivalent zanamivir were much higher against A/Bayern/63/2009 (H1N1pdm) virus than against the tested H3N2 viruses, implying a decreased zanamivir sensitivity of this virus. Importantly, the heteromultivalent compounds were able to overcome this decreased zanamivir sensitivity, suggesting they might be suited to treat infections with NA inhibitor-resistant viruses as well. Overall, the heteromultivalent compound with both ZA and SL ligands, $LPG_{10}ZA_{0.40}SL_{0.40,}$ was the most effective compound accomplishing >99.9% inhibition of virus propagation against the diverse influenza A viruses tested, demonstrating its high potential for broad activity (**Figure 2A-C**). Important to note is that the presence of ZA-NA pairs on the virus surface might also stabilize HA-SL pairs, leading to long-lasting adsorption of heteromultivalent $LPG_{10}ZA_{0.40}SL_{0.40}$ and consequently better steric inhibition of the virus surface compared to its homomultivalent analogs.

To investigate if there was an added benefit of having both SA and ZA on a single polymer backbone in contrast to separate ones, a comparison of covalently bound heteromultivalent compound $LPG_{10}ZA_{0.10}SA_{0.40}$ with the physical mixture of $LPG_{10}ZA_{0.10}$ and $LPG_{10}SA_{0.40}$ was also performed in the multicyclic infection setup at a low inhibitor concentration of 10 nM. The $LPG_{10}ZA_{0.10}SA_{0.40}$ at 10 nM corresponds to ZA and SA concentrations of 130 nM and 530 nM,

respectively. A physical mixture containing 130 nM (ZA concentration) $LPG_{10}ZA_{0.10}$ and 530 nM (SA concentration) $LPG_{10}SA_{0.40}$ was used in the same experimental setting. The virus titer was determined by plaque assay at 24 hpi using MDCK-II cells. We observed for the influenza viruses A/X31 (H3N2), A/Bremen/5/2017 (H3N2) and A/PR/8/34 (H1N1) that the heteromultivalent compound reduced the virus titer by one order of magnitude more than the physical mixture of the analogs at 10 nM concentrations (**Figure 2D**). The lower effect of physical mixtures might be attributed to the shielding effect posed by the homomultivalent analog once bound to the virus particle. For example, LPGSA once bound to the virus particle might also shield NAs and make them less accessible to binding with LPGZA analogs and vice versa. However, this warrants more detailed studies in the future. Importantly, all compounds did not show any toxicity against MDCK-II cells in MTS assay up to 10 µM concentration (**Figure S19**).

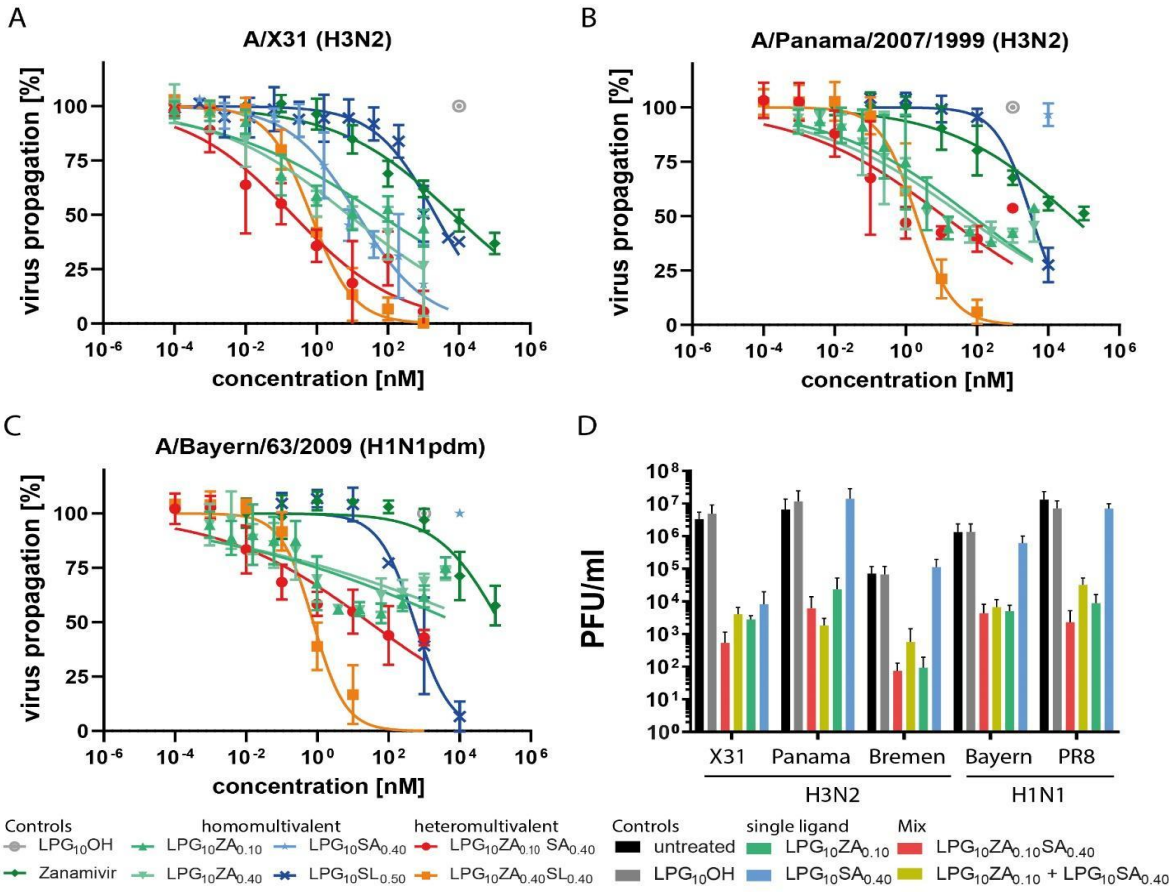

Figure 2. Investigation of different compounds in a multicyclic infection set up against different strains of influenza A virus. **Figures A**, **B** and **C** show the reduction in the virus titer in presence of different compounds at different concentrations against the influenza viruses A/X31 (H3N2), A/Panama/2007/1999 (H3N2), and A/Bayern/63/ 2009 (H1N1pdm), respectively. IC_{50} values in **Table 2** were calculated from these curves using a 4^{th}-order non-linear regression fit in Graphpad Prism. **Figure D** shows a reduction in virus titers of different strains (additionally including A/Bremen/5/2017 (H3N2) and A/PR/8/34 (H1N1)) at 10 nM of the compound using homomultivalent ZA and SA compounds as well as the physical mixture of homomultivalent LPG to compare to covalently bound heteromultivalent ligands. Only the location names are used to refer to the different strains for clarity. All data represent three independent experiments in duplicates.

Table 2. Inhibition of propagation of diverse IAV virus strains in cell culture by different compounds. All compounds were added to the culture medium directly after 45 min of infection at MOI 0.01. IC_{50} values were calculated by fitting the data from **Figure 2A-C** using a 4^{th}-order nonlinear regression. IC_{50} values are given as particle concentrations. In addition, the concentrations of the respective ligands are given in brackets.

Compounds	**IC_{50} ± SD [nM] (SA, ZA)**		
	A/X31 (H3N2)	**A/Panama/2007/2009 (H3N2)**	**A/Bayern/63/2009 (H1N1)**
$LPG_{10}OH$	-	-	-
$LPG_{10}SA_{0.40}$	31.17 ±38.36 (SA: 1870)	ND	ND
$LPG_{10}SL_{0.50}$	2841.67 ± 1223.89 (SL: 190 391)	2400.33 ± 1475.07 (SL: 160 822)	648.23 ± 459.69 (SL: 43 431)
Zanamivir	7282.00 ± 3733.91	9886.67 ± 5838.55	6537.00 ± 9244.71
$LPG_{10}ZA_{0.10}$	5.88 ± 3.02 (ZA: 76)	58.46 ± 22.62 (ZA: 760)	$(7.72 \pm 7.44) \times 10^4$ (ZA:1000 000)
$LPG_{10}ZA_{0.40}$	3.35 ± 0.57 (ZA: 181)	45.47 ± 26.57 (ZA: 2455)	$(1.40 \pm 1.71) \times 10^4$ (ZA:756 000)
$LPG_{10}ZA_{0.10}SA_{0.40}$	0.15 ± 0.08 (ZA: 2, SA: 9)	26.16 ± 38.21 (ZA: 340, SA: 1569)	156.18 ±246.41 (ZA:2030, SA: 9370)
$LPG_{10}ZA_{0.40}SL_{0.40}$	0.65 ± 0.36 (ZA, SL:35)	2.37 ± 2.24 (ZA, SL:128)	0.86 ± 0.48 (ZA, SL:46)

ND: not detected

Also, we imaged cells at 24 hpi with A/X31 (H3N2) virus in presence of different inhibitors. Influenza A/X31 (H3N2) viral nucleoproteins (NP) were labeled with antibodies to reveal infected cells and DAPI staining of nuclei was used to mark the cells. Representative images are shown in **Figure 3A** and **Figure S20**. In the infection control (absence of any LPG compound) and $LPG_{10}OH$ treated cells, nearly all the cells were infected within 24 hpi (MOI= 0.01). Upon adding polymeric inhibitors to the cell culture medium directly after 45 min of infection, the number of infected cells became substantially reduced. The heteromultivalent compound $LPG_{10}ZA_{0.40}SL_{0.40}$ showed the best inhibitory activity among all the compounds, and its activity was significantly higher than the two homomultivalent inhibitors ($LPG_{10}ZA_{0.40}$ and $LPG_{10}SA_{0.40}$). Similar to the IC_{50} analysis, we saw higher antiviral activities for multivalent zanamivir compounds ($LPG_{10}ZA_{0.10}$ and $LPG_{10}ZA_{0.40}$) over monomeric zanamivir. These findings both rationalize the efficient anti-influenza efficacy of polymeric inhibitors and demonstrate that attaching both HA and NA inhibitors to the same polymeric chain confers additional benefits for inhibiting virus propagation even post-infection. Since the cells had been infected for 45 min before the treatment by inhibitors, the observation of fewer infected cells indicates that the viral spread in the culture was reduced.

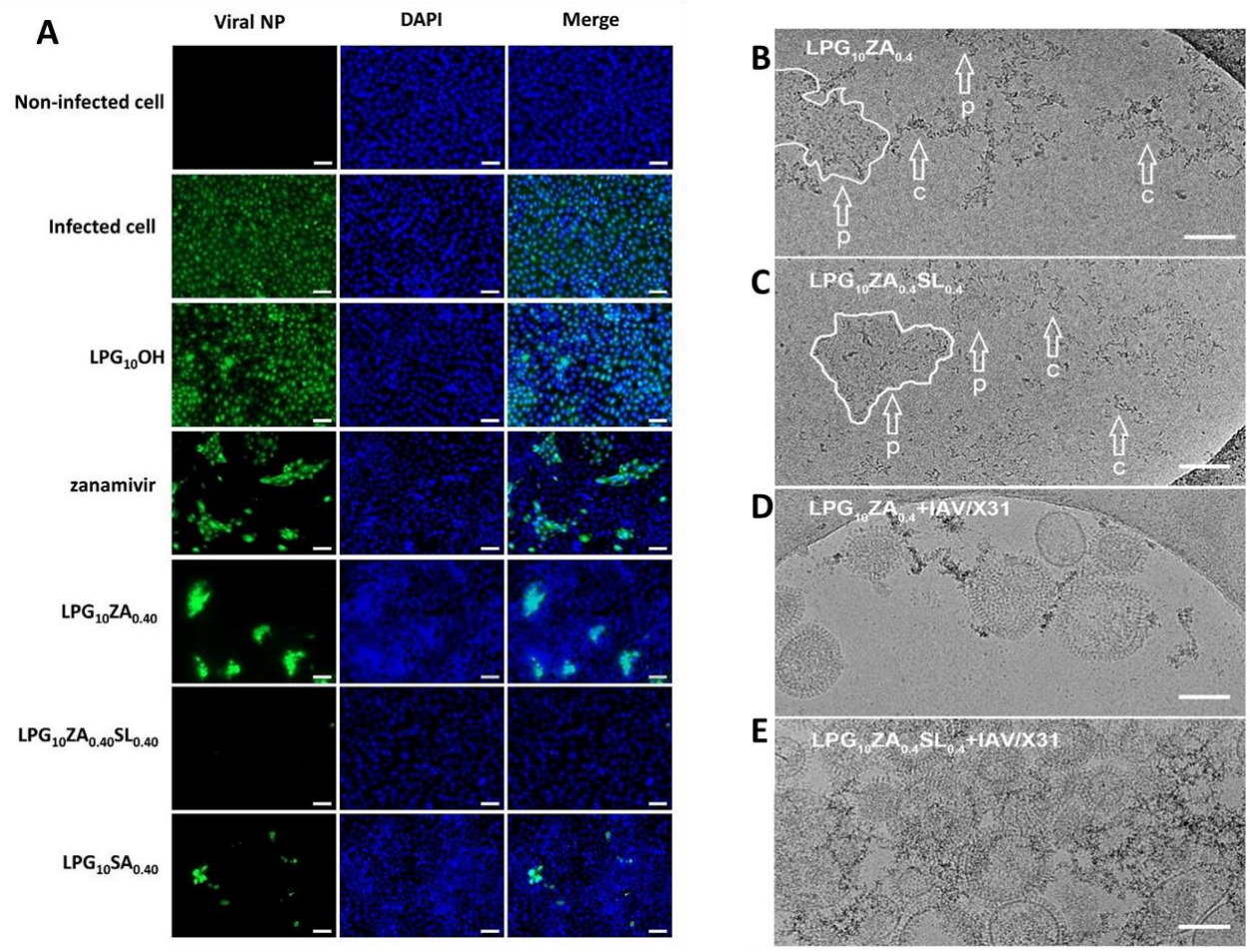

Figure 3. (A) Representative fluorescent images for infected cells being treated with the inhibitors. The cells were infected by IAV A/X31 (H3N2) for 45 min and then cultured in the medium containing 10 nM inhibitors for 24 hours. Scale bar: 50 μm. Immunostaining was done for the viral nucleoprotein (NP). More images are shown in **Figure S21**. Morphology of (B) $LPG_{10}ZA_{0.40}$ and (C) $LPG_{10}ZA_{0.40}SL_{0.40}$ (1 mM) embedded in vitreous ice. Arrows in (B) and (C) indicate condensed LPG structures (=c) or planar 2D structures (=p), the latter partly outlined with a line. Cryo-electron micrograph of (D) $LPG_{10}ZA_{0.40}$ and (E) $LPG_{10}ZA_{0.40}SL_{0.40}$ incubated with IAV A/X31 (H3N2) in PBS pH 7.4 for 45 min at room temperature and embedded in vitreous ice. The scale bar corresponds to 100 nm.

To visualize the IAV interactions, we did cryo-TEM imaging with different compounds at 1mM concentrations and seasonal influenza A/X31 (H3N2) virus (See Supporting Information **Figure S12-S16**). The $LPG_{10}ZA_{0.10}$ showed clusters of thread-like structures and some 2D planar morphologies that were particularly evident in micrographs taken using a contrast-enhancing volta

phase plate (**Figure 3B**, **Figure S12**). The 2D planar morphologies were much more prominent in $LPG_{10}ZA_{0.40}$ with increased loading of ZA ligand that has both a positively charged guanidinium and a negatively charged carboxylate ion. The $LPG_{10}ZA_{0.40}$ carries a more negative zeta potential (-17.41±3.48 mV) than $LPG_{10}ZA_{0.10}$ (ζ = -3.31±1.40 mV) (**Table 1** and **Figure S13-S14**). but less negative than the $LPG_{10}SA_{0.40}$ (ζ = -30 mV). We hypothesize the electrostatic interactions among different polymer chains to be the main cause of the formation of 2D planar morphologies. The multivalent sialyllactose compound $LPG_{10}SL_{0.50}$ showed only some punctual or thread morphologies which could be particularly well recognized in stereo images (**Figure S16**). On the other hand, the heteromultivalent compound $LPG_{10}ZA_{0.40}SL_{0.40}$ also showed easily recognizable 2D planar morphologies attributed to the presence of high ZA loading (**Figure 3C** and **Figure S15**).

We incubated the two most potent compounds $LPG_{10}ZA_{0.40}$ and $LPG_{10}ZA_{0.40}SL_{0.40}$ with influenza A virus A/X31 (H3N2) and plunge froze them for cryo-TEM study. Interestingly, in the presence of the virus, 2D planar morphologies could not be recognized. The disruption of 2D structures might be because of the higher affinity of carbohydrate ligands towards viral proteins as compared to their potential electrostatic interactions among the ligands. Some clusters of $LPG_{10}ZA_{0.40}$ in the vicinity of virions could be seen as shown in **Figure 3D** and **Figure S17**. In the presence of the most potent heteromultivalent compound $LPG_{10}ZA_{0.40}SL_{0.40}$, we observed a high virus density often surrounded by compound clusters, suggesting compound-mediated aggregation of virus particles (**Figure 3E** and **Figure S18**). This clustering effect may contribute to the efficient inhibition of virus propagation observed *in vitro* (**Figures 1** and **2**) and *ex vivo* (**Figure 4**).

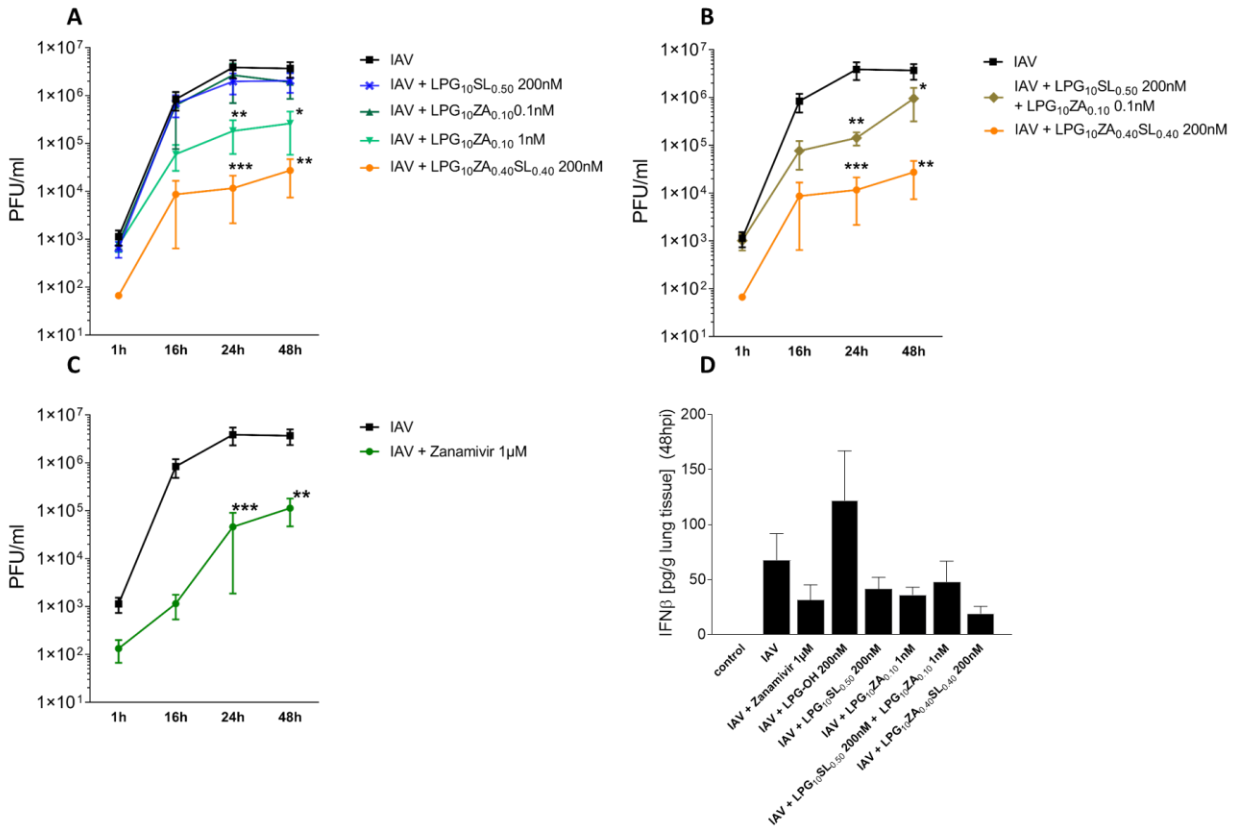

Figure 4. Inhibition of *ex vivo* human lung tissue influenza A virus A/Panama/2007/1999 (H3N2) propagation with different compounds. IAV (black) replication was compared to the replication after treatment with (A) $LPG_{10}SL_{0.50}$ (blue), $LPG_{10}ZA_{0.10}$ (green) or $LPG_{10}ZA_{0.40}SL_{0.40}$ (orange), (B) $LPG_{10}SL_{0.50}$ + $LPG_{10}ZA_{0.10}$ (brown) and $LPG_{10}ZA_{0.40}SL_{0.40}$ (orange) or (C) zanamivir (green). (D) The released IFN-β was measured at 48 hpi. Control is the sample without any virus where no detectable IFN-β was released. Data are presented as mean with SEM (N=4). Data were analyzed using a Two-Way ANOVA (*p<0.05, **p<0.01 ***p<0.001, Dunnett's multiple comparisons test).

To mimic the natural setting of the human lung more closely, virus infections were studied in explanted human lung tissue infected *ex vivo*. Compounds were administered only once at 1.5 hpi with IAV/Panama/2007/1999 (H3N2) virus (0.4 x 10^6 PFU/mL) and plaque-forming units (PFU) in the supernatants of infected human lung tissue were assessed at 16, 24, and 48 hpi, respectively. Importantly, the concentrations of different compounds with different degrees of functionalization were based on the previous *in vitro* assays and *ex vivo* optimization. A comparison of $LPG_{10}SL_{0.50}$

at 100 and 200 nM showed that at least 200 nM concentration was required to observe a slight reduction in the virus titer (See supporting information **Figure S21**). Similarly, $LPG_{10}ZA_{0.10}$ at 1 nM reduced the virus titer up to one order of magnitude within 48 hpi whereas the 0.1 nM concentration was only slightly effective in this *ex vivo* setup. Interestingly, the physical mixture of 0.1 nM $LPG_{10}ZA_{0.10}$ and 200 nM $LPG_{10}SL_{0.50}$ reduced the virus titer up to one order at 16 and 24 hours, but the virus infectivity was restored within 48 hpi. The most effective was the heteromultivalent $LPG_{10}ZA_{0.40}SL_{0.40}$ which significantly reduced the virus titer almost up to three orders of magnitude and a plateau in PFU was reached at 16 hpi at 200 nM. Commercially available ZA was initially able to reduce virus titers when applied at µM concentration although virus titers continued to rise steadily without reaching a plateau within 48 hpi (**Figure 4A-C**).

Taken together, the heteromultivalent compound $LPG_{10}ZA_{0.40}SL_{0.40}$ outperformed even physical mixtures of the highly active homomultivalent ZA and the homomultivalent SL compounds *ex vivo*. This indicates a synergistic effect of weakly active ligands covalently bound to the same polymer backbone, which could not be achieved by using mere physical mixtures. As expected, the unfunctionalized control compound $LPG_{10}OH$ without any ligand did not have any significant inhibition (**Figure S21**).

As a representative of antiviral cytokine release from the infected cells at 48 hpi, we measured the level of IFN-β using ELISA. Notably, the levels of IFN-β were substantially reduced in the infected tissue cultures treated with monovalent ZA, homomultivalent, or heteromultivalent compounds. Furthermore, the IFN-β reduction was even more pronounced in the presence of the heteromultivalent compounds compared to the other multivalent compounds or ZA alone (**Figure 4D**). Considering IFN-β as representative interferon allows the assumption that the high antiviral

activity of heteromultivalent compounds is mediated by their binding to viruses and not by cytokine induction.

In conclusion, the heteromultivalent polymer carrying SL and ZA units exhibits significantly higher antiviral effects than their homomultivalent analogs. It is also effective against those IAV strains for which the homomultivalent compounds show little to no effect, suggesting a potential application also against NA inhibitor-resistant strains. Overall, the data show that the high efficacy of the heteromultivalent polymer is not solely because of binding with two different proteins onto the virus surface but is a result of better polymer adsorption and steric inhibition of the virus surface. The most potent $LPG_{10}ZA_{0.40}SL_{0.40}$ inhibits propagation of a broad variety of IAV strains up to >99.9% post-infection at a very low nanomolar concentration and outperforms the commercial zanamivir drug in cell culture assays as well as in the human lung infection model. We demonstrate that the dual-action approach can be integrated into a small multivalent polymer, and it possesses a high potential to advance our options to combat influenza virus infections. This approach may also be applicable to combat infections with other viruses anchoring specialized surface proteins.

Supporting Information

Supporting Information is available free of charge at ACS Publications website.

AUTHOR INFORMATION

Corresponding Author

*Sumati Bhatia - Institut für Chemie und Biochemie Organische Chemie, Freie Universität Berlin, Takustr. 3, 14195 Berlin, Germany

Email: sumati@zedat.fu-berlin.de

ACKNOWLEDGEMENTS

B.P. and M.S. contributed equally to this work. The authors acknowledge financial support by the Collaborative Research Center 765 and 1449 of the Deutsche Forschungsgemeinschaft (DFG) and Berlin University Alliance (BUA). S.B. is funded from DFG – Projektnummer 458564133. K.H. and A.C.H. were supported by DFG (SFB-TR 84). K.H. and A.C.H. were funded by BMBF (NUM-COVID 19, Organo-Strat 01KX2021), A.C.H. was funded by BMBF (RAPID) and by Berlin University Alliance GC2 Global Health (Corona Virus Pre-Exploration Project). M.B., K.H. and A.C.H. were supported by Einstein Foundation EC3R. We acknowledge Stefan Hippenstiel for his valuable advice on HuLu experiments.

Funding sources

Einstein Foundation EC3R, BMBF (RAPID, NUM-COVID 19, Organo-Strat 01KX2021), DFG (SFB-TR 84), BIH and Charité-Zeiss MultiDim, DFG (Projektnummer 458564133), DFG (SFB-765 and 1449), BUA corona virus Pre-exploration Project

Notes

The authors declare no conflict of interest.

References

(1) https://www.who.int/news-room/fact-sheets/detail/influenza-(seasonal). *World Health Organization. Influenza (Seasonal)*.

(2) Bai, L.; Zhao, Y.; Dong, J.; Liang, S.; Guo, M.; Liu, X.; Wang, X.; Huang, Z.; Sun, X.; Zhang, Z.; Dong, L.; Liu, Q.; Zheng, Y.; Niu, D.; Xiang, M.; Song, K.; Ye, J.; Zheng, W.; Tang, Z.; Tang, M.; Zhou, Y.; Shen, C.; Dai, M.; Zhou, L.; Chen, Y.; Yan, H.; Lan, K.; Xu, K. Coinfection with Influenza A Virus Enhances SARS-CoV-2 Infectivity. *Cell Res* **2021**, *31* (4), 395–403. https://doi.org/10.1038/s41422-021-00473-1.

(3) Cuadrado-Payán, E.; Montagud-Marrahi, E.; Torres-Elorza, M.; Bodro, M.; Blasco, M.; Poch, E.; Soriano, A.; Piñeiro, G. J. SARS-CoV-2 and Influenza Virus Co-Infection. *Lancet* **2020**, *395* (10236), e84. https://doi.org/10.1016/S0140-6736(20)31052-7.

(4) Stowe, J.; Tessier, E.; Zhao, H.; Guy, R.; Muller-Pebody, B.; Zambon, M.; Andrews, N.; Ramsay, M.; Lopez Bernal, J. Interactions between SARS-CoV-2 and Influenza, and the Impact of Coinfection

on Disease Severity: A Test-Negative Design. *Int J Epidemiol* **2021**, *50* (4), 1124–1133. https://doi.org/10.1093/ije/dyab081.

(5) de Vries, E.; Du, W.; Guo, H.; de Haan, C. A. M. Influenza A Virus Hemagglutinin–Neuraminidase–Receptor Balance: Preserving Virus Motility. *Trends Microbiol* **2020**, *28* (1), 57–67. https://doi.org/10.1016/j.tim.2019.08.010.

(6) Vahey, M. D.; Fletcher, D. A. Influenza A Virus Surface Proteins Are Organized to Help Penetrate Host Mucus. *Elife* **2019**, *8*. https://doi.org/10.7554/eLife.43764.

(7) Hamming, P. H. (Erik); Overeem, N. J.; Huskens, J. Influenza as a Molecular Walker. *Chem Sci* **2020**, *11* (1), 27–36. https://doi.org/10.1039/C9SC05149J.

(8) McAuley, J. L.; Gilbertson, B. P.; Trifkovic, S.; Brown, L. E.; McKimm-Breschkin, J. L. Influenza Virus Neuraminidase Structure and Functions. *Front Microbiol* **2019**, *10*. https://doi.org/10.3389/fmicb.2019.00039.

(9) Burckhardt, C. J.; Greber, U. F. Virus Movements on the Plasma Membrane Support Infection and Transmission between Cells. *PLoS Pathog* **2009**, *5* (11), e1000621. https://doi.org/10.1371/journal.ppat.1000621.

(10) Overeem, N. J.; Vries, E.; Huskens, J. A Dynamic, Supramolecular View on the Multivalent Interaction between Influenza Virus and Host Cell. *Small* **2021**, *17* (13), 2007214. https://doi.org/10.1002/smll.202007214.

(11) Vahey, M. D.; Fletcher, D. A. Influenza A Virus Surface Proteins Are Organized to Help Penetrate Host Mucus. *Elife* **2019**, *8*. https://doi.org/10.7554/eLife.43764.

(12) Sieben, C.; Kappel, C.; Zhu, R.; Wozniak, A.; Rankl, C.; Hinterdorfer, P.; Grubmüller, H.; Herrmann, A. Influenza Virus Binds Its Host Cell Using Multiple Dynamic Interactions. *Proceedings of the National Academy of Sciences* **2012**, *109* (34), 13626–13631. https://doi.org/10.1073/pnas.1120265109.

(13) Cohen, M.; Zhang, X.-Q.; Senaati, H. P.; Chen, H.-W.; Varki, N. M.; Schooley, R. T.; Gagneux, P. Influenza A Penetrates Host Mucus by Cleaving Sialic Acids with Neuraminidase. *Virol J* **2013**, *10* (1), 321. https://doi.org/10.1186/1743-422X-10-321.

(14) von Itzstein, M.; Dyason, J. C.; Oliver, S. W.; White, H. F.; Wu, W.-Y.; Kok, G. B.; Pegg, M. S. A Study of the Active Site of Influenza Virus Sialidase: An Approach to the Rational Design of Novel Anti-Influenza Drugs. *J Med Chem* **1996**, *39* (2), 388–391. https://doi.org/10.1021/jm950294c.

(15) Trebbien, R.; Pedersen, S. S.; Vorborg, K.; Franck, K. T.; Fischer, T. K. Development of Oseltamivir and Zanamivir Resistance in Influenza A(H1N1)Pdm09 Virus, Denmark, 2014. *Eurosurveillance* **2017**, *22* (3). https://doi.org/10.2807/1560-7917.ES.2017.22.3.30445.

(16) Mammen, M.; Dahmann, G.; Whitesides, G. M. Effective Inhibitors of Hemagglutination by Influenza Virus Synthesized from Polymers Having Active Ester Groups. Insight into Mechanism of Inhibition. *J Med Chem* **1995**, *38* (21), 4179–4190. https://doi.org/10.1021/jm00021a007.

(17) Kwon, S.-J.; Na, D. H.; Kwak, J. H.; Douaisi, M.; Zhang, F.; Park, E. J.; Park, J.-H.; Youn, H.; Song, C.-S.; Kane, R. S.; Dordick, J. S.; Lee, K. B.; Linhardt, R. J. Nanostructured Glycan Architecture Is Important in the Inhibition of Influenza A Virus Infection. *Nat Nanotechnol* **2017**, *12* (1), 48–54. https://doi.org/10.1038/nnano.2016.181.

(18) Papp, I.; Sieben, C.; Ludwig, K.; Roskamp, M.; Böttcher, C.; Schlecht, S.; Herrmann, A.; Haag, R. Inhibition of Influenza Virus Infection by Multivalent Sialic-Acid-Functionalized Gold Nanoparticles. *Small* **2010**, *6* (24), 2900–2906. https://doi.org/10.1002/smll.201001349.

(19) Lauster, D.; Klenk, S.; Ludwig, K.; Nojoumi, S.; Behren, S.; Adam, L.; Stadtmüller, M.; Saenger, S.; Zimmler, S.; Hönzke, K.; Yao, L.; Hoffmann, U.; Bardua, M.; Hamann, A.; Witzenrath, M.; Sander, L. E.; Wolff, T.; Hocke, A. C.; Hippenstiel, S.; de Carlo, S.; Neudecker, J.; Osterrieder, K.; Budisa, N.; Netz, R. R.; Böttcher, C.; Liese, S.; Herrmann, A.; Hackenberger, C. P. R. Phage Capsid Nanoparticles with Defined Ligand Arrangement Block Influenza Virus Entry. *Nat Nanotechnol* **2020**, *15* (5), 373–379. https://doi.org/10.1038/s41565-020-0660-2.

(20) Bhatia, S.; Hilsch, M.; Cuellar-Camacho, J. L.; Ludwig, K.; Nie, C.; Parshad, B.; Wallert, M.; Block, S.; Lauster, D.; Böttcher, C.; Herrmann, A.; Haag, R. Adaptive Flexible Sialylated Nanogels as Highly Potent Influenza A Virus Inhibitors. *Angewandte Chemie International Edition* **2020**, *59* (30), 12417–12422. https://doi.org/10.1002/anie.202006145.

(21) Kumari, M.; Prasad, S.; Fruk, L.; Parshad, B. Polyglycerol-Based Hydrogels and Nanogels: From Synthesis to Applications. *Future Med Chem* **2021**, *13* (4), 419–438. https://doi.org/10.4155/fmc-2020-0205.

(22) Wang, H.; Huang, W.; Orwenyo, J.; Banerjee, A.; Vasta, G. R.; Wang, L.-X. Design and Synthesis of Glycoprotein-Based Multivalent Glyco-Ligands for Influenza Hemagglutinin and Human Galectin-3. *Bioorg Med Chem* **2013**, *21* (7), 2037–2044. https://doi.org/10.1016/j.bmc.2013.01.028.

(23) Sauter, N. K.; Bednarski, M. D.; Wurzburg, B. A.; Hanson, J. E.; Whitesides, G. M.; Skehel, J. J.; Wiley, D. C. Hemagglutinins from Two Influenza Virus Variants Bind to Sialic Acid Derivatives with Millimolar Dissociation Constants: A 500-MHz Proton Nuclear Magnetic Resonance Study. *Biochemistry* **1989**, *28* (21), 8388–8396. https://doi.org/10.1021/bi00447a018.

(24) Stadtmueller, M. N.; Bhatia, S.; Kiran, P.; Hilsch, M.; Reiter-Scherer, V.; Adam, L.; Parshad, B.; Budt, M.; Klenk, S.; Sellrie, K.; Lauster, D.; Seeberger, P. H.; Hackenberger, C. P. R.; Herrmann, A.; Haag, R.; Wolff, T. Evaluation of Multivalent Sialylated Polyglycerols for Resistance Induction in and Broad Antiviral Activity against Influenza A Viruses. *J Med Chem* **2021**, *64* (17), 12774–12789. https://doi.org/10.1021/acs.jmedchem.1c00794.

(25) Bhatia, S.; Lauster, D.; Bardua, M.; Ludwig, K.; Angioletti-Uberti, S.; Popp, N.; Hoffmann, U.; Paulus, F.; Budt, M.; Stadtmüller, M.; Wolff, T.; Hamann, A.; Böttcher, C.; Herrmann, A.; Haag, R. Linear Polysialoside Outperforms Dendritic Analogs for Inhibition of Influenza Virus Infection in Vitro and in Vivo. *Biomaterials* **2017**, *138*, 22–34. https://doi.org/10.1016/j.biomaterials.2017.05.028.

(26) Thomas, A.; Müller, S. S.; Frey, H. Beyond Poly(Ethylene Glycol): Linear Polyglycerol as a Multifunctional Polyether for Biomedical and Pharmaceutical Applications. *Biomacromolecules* **2014**, *15* (6), 1935–1954. https://doi.org/10.1021/bm5002608.

(27) Vahey, M. D.; Fletcher, D. A. Low-Fidelity Assembly of Influenza A Virus Promotes Escape from Host Cells. *Cell* **2019**, *176* (1–2), 281-294.e19. https://doi.org/10.1016/j.cell.2018.10.056.

(28) Harris, A.; Cardone, G.; Winkler, D. C.; Heymann, J. B.; Brecher, M.; White, J. M.; Steven, A. C. Influenza Virus Pleiomorphy Characterized by Cryoelectron Tomography. *Proceedings of the National Academy of Sciences* **2006**, *103* (50), 19123–19127. https://doi.org/10.1073/pnas.0607614103.

(29) Masuda, T.; Yoshida, S.; Arai, M.; Kaneko, S.; Yamashita, M.; Honda, T. Synthesis and Anti-Influenza Evaluation of Polyvalent Sialidase Inhibitors Bearing 4-Guanidino-Neu5Ac2en Derivatives. *Chem Pharm Bull (Tokyo)* **2003**, *51* (12), 1386–1398. https://doi.org/10.1248/cpb.51.1386.

(30) Varilly, P.; Angioletti-Uberti, S.; Mognetti, B. M.; Frenkel, D. A General Theory of DNA-Mediated and Other Valence-Limited Colloidal Interactions. *J Chem Phys* **2012**, *137* (9), 094108. https://doi.org/10.1063/1.4748100.

(31) Angioletti-Uberti, S.; Varilly, P.; Mognetti, B. M.; Tkachenko, A. v.; Frenkel, D. Communication: A Simple Analytical Formula for the Free Energy of Ligand–Receptor-Mediated Interactions. *J Chem Phys* **2013**, *138* (2), 021102. https://doi.org/10.1063/1.4775806.

(32) de Graaf, M.; Fouchier, R. A. M. Role of Receptor Binding Specificity in Influenza A Virus Transmission and Pathogenesis. *EMBO J* **2014**, *33* (8), 823–841. https://doi.org/10.1002/embj.201387442.

(33) Hatakeyama, S.; Sakai-Tagawa, Y.; Kiso, M.; Goto, H.; Kawakami, C.; Mitamura, K.; Sugaya, N.; Suzuki, Y.; Kawaoka, Y. Enhanced Expression of an A2,6-Linked Sialic Acid on MDCK Cells Improves Isolation of Human Influenza Viruses and Evaluation of Their Sensitivity to a Neuraminidase Inhibitor. *J Clin Microbiol* **2005**, *43* (8), 4139–4146. https://doi.org/10.1128/JCM.43.8.4139-4146.2005.

(34) Lees, W. J.; Spaltenstein, A.; Kingery-Wood, J. E.; Whitesides, G. M. Polyacrylamides Bearing Pendant .Alpha.-Sialoside Groups Strongly Inhibit Agglutination of Erythrocytes by Influenza A Virus: Multivalency and Steric Stabilization of Particulate Biological Systems. *J Med Chem* **1994**, *37* (20), 3419–3433. https://doi.org/10.1021/jm00046a027.

(35) Ponader, D.; Maffre, P.; Aretz, J.; Pussak, D.; Ninnemann, N. M.; Schmidt, S.; Seeberger, P. H.; Rademacher, C.; Nienhaus, G. U.; Hartmann, L. Carbohydrate-Lectin Recognition of Sequence-Defined Heteromultivalent Glycooligomers. *J Am Chem Soc* **2014**, *136* (5), 2008–2016. https://doi.org/10.1021/ja411582t.